Journal of Physics:
Conference Series

PAPER • **OPEN ACCESS**

Study on the influence of expansion waves on the reflection type of shock wave in double-wedge configurations

To cite this article: Liyao Wang *et al* 2024 *J. Phys.: Conf. Ser.* **2882** 012025

Journal of Physics: Conference Series **2882** (2024) 012025 doi:10.1088/1742-6596/2882/1/012025

Study on the influence of expansion waves on the reflection type of shock wave in double-wedge configurations

Liyao Wang[1,2], Li Yang[1,2,*] and Lianjie Yue[2]

[1]School of Aeronautics, Chongqing Jiaotong University, Chongqing 402247, China
[2]State Key Laboratory of High Temperature Gas Dynamics, Institute of Mechanics, Chinese Academy of Sciences, Beijing 100190, China

[*]Corresponding author's e-mail: yangli991@hotmail.com

Abstract. This paper investigates how variations in the relative positioning between the expansion fan emitted from the triple point in the shock/shock interference on double-wedge geometries in confined spaces and the incidence point of oblique shocks influence the transition of oblique shock reflection types, and understands the roles of expansion waves in inhibiting MR. Predictive analysis through the shock polar line provides critical values for the transition of oblique shock reflection types under the influence of expansion fan effects. The position where the shock/expansion fan undergoes post-oblique reflection on the opposite sidewall can be controlled by adjusting the model's contraction ratio (H_1/H_2). This study uses the density-based solver blastFOAM in openFOAM to numerically solve the Euler equations, conducting inviscid calculations of shock/shock interactions induced by double wedges in confined spaces with ideal gases. This study compares pressure values in different regions obtained from numerical simulations and examines the reflection types of oblique shocks on opposite sidewalls, confirming the feasibility of shock polar analysis and the accuracy of theoretical predictions.

1. Introduction

The shock/shock interaction represents critical issues that have been extensively studied in the field of hypersonic flight [1,2]. Such interactions may create complex shock structures, affecting engine inlet compression efficiency, potentially leading to increased local thermal and pressure loads on the aircraft surface and significant oscillations in the flow field, thereby influencing the aerodynamic design performance of the aircraft. To ensure the operational performance of the inlet under hypersonic flight conditions, this study focuses on the simplified model of the inlet of a hypersonic air-breathing propulsion system - confined space double wedges. It examines the reflection flow field structure induced by the double wedges through shock polar analysis and numerical studies [3,4].

Since Edney [5] proposed a classification criterion for shock/shock interaction, the phenomenon of shock/shock interaction has been widely studied [6,7]. The Type I and Type VI shock/shock interactions induced by double wedges, due to their typical wave structure, have been observed to significantly affect aircraft in numerous experimental studies [8,9], and they have become focal points in numerical research [10].

Olejniczak et al. [11] numerically investigated inviscid structures of double wedge flows under supersonic conditions, and a criterion of the transition between Type I-VI shock/shock interaction is proposed for different freestream Mach numbers and deflection angles. Specifically, Type VI interaction occurs between two oblique shocks on the same side, with an expansion fan emitted at the triple point

incident on the wall, and the expansion fan influences shock reflection types in confined spaces.

The interaction of two oblique shocks in a double wedge generates complex wave structures, where shocks and expansion waves respectively promote/inhibit MR on the wall of confined spaces. However, little research focused on shock/shock interactions induced by confined-space double wedge. Guan et al. [12,13] studied the reflection and interaction flow field of dual-oblique-shocks, highlighting a bistable region with Type I or Type II shock wave interference in the pre-Mach reflection (MR) flow field, and two distinct jets were captured after Mach stem.

This paper utilizes shock polar analysis to investigate the influence of expansion waves on the reflection types of oblique shocks in Type VI interference. It establishes criteria for the transition of oblique shock reflection types on opposite walls. The study conducts inviscid numerical research into shock interactions induced by confined space double wedges, exploring the impact of expansion fans from triple points where shocks intersect under conditions of θ_1=8°, θ_2=26°, and Ma=4.5.

2. Numerical and theoretical methods

The two-dimensional compressible Euler equations are solved using a finite-volume computational fluid dynamics method.

The formulation is given as follows:

$$\frac{\partial Q}{\partial t}+\frac{\partial F}{\partial x}(F_1)+\frac{\partial F}{\partial y}(F_2)=0 \tag{1}$$

$$Q=\begin{bmatrix}\rho\\ \rho u\\ \rho \upsilon\\ e\end{bmatrix},\quad F_1=\begin{bmatrix}\rho u\\ \rho u^2+p\\ \rho \upsilon\\ (e+p)u\end{bmatrix},F_2=\begin{bmatrix}\rho u\\ \rho u\\ \rho \upsilon^2+p\\ (e+p)v\end{bmatrix}$$

where ρ denotes the total density, p is the pressure, e is the energy of the mixture; u and v are the velocities in the x and y directions.

This paper uses the ideal gas state equation which is given as follows:

$$p=\rho RT \tag{2}$$

where R denotes the molar mass, and T denotes the thermodynamic temperature.

The free stream is supersonic the inflow conditions are specified, and the grid is chosen so that the outflow is also supersonic. Thus, simple zeroth-order extrapolation of the variables at the outflow is appropriate. At the wedge surfaces, we set a slip wall.

3. Results and discussion

3.1 Shock polar analysis considering the effects of expansion waves

To predict the reflection types of incident shocks with the effects of expansion fans, a shock polar that can determine the possible flow states with a given inflow condition is performed. The intersection point of the shock polar line in Figure 2 corresponds to the region labels of the flow field schematic in Figure 1.

For the freestream Ma=4.5, the post-shock state (1) after the oblique shock AC in Figure 2 is determined at Point (1) on the shock polar R_1 with deflection angle θ_1=8°. Point (2) corresponds to the post-shock state (2) after oblique shock BC, which is located on the shock polar R_2 emanate from Point (1). Due to Region (3) after EF and Region (4) after oblique shock CG divided by the slip line CD, the same pressure of both regions is needed. Therefore, Points (3, 4) are located at the intersection of curved line EF starting from Point (2) and the shock polar R_2, and the polar line R_7, starting from Points (3, 4), reflects the reflection type of oblique shock CG before ReEF. Region (5) behind the reflected expansion fan ReEF meets the requirement that the streamline across shock CG should parallel to the trailing edge. Point (5) places on shock polar R_1 with deflection angle θ_2. The polar line R_8, starting from Point (5), reflects the reflection type of oblique shock CG after the ReEF.

The position relationship between the incident shock CG and the expansion fan is different with varied C_r, which is the model's contraction ratio (H_1/H_2). In Figure 1(a), ReEF acts downstream of the incident shock CG, resulting in the corresponding post-shock states (3, 4) as shown in Figure 2(a). In Figure 1(b), the ReEF acts upstream of the incident shock CG, resulting in the corresponding post-shock state (5) as shown in Figure 2(a). For the typical wave configuration in Figure 1(a), the Polar line R_7 originated from Point (3, 4) in Figure 2(a) is tangent with θ=0, which is the critical condition between the dual-solution region and Mach reflection region. Due to the influence of the expansion fan, R_8 transitions into R_7, representing a critical condition upstream of the expansion wave, and the deflection angle θ_2 is denoted as $\theta_{D(4)}$. As the deflection angle θ_2 increases, the shock polar lines evolve as shown in Figure 2(b). The deflection angle θ_2 in this scenario is denoted as $\theta_{D(5)}$. When $\theta_{D(4)} < \theta_2 < \theta_{D(5)}$, varying C_r controls the relative position between the expansion fan and the shock inlet point, allowing the flow states corresponding to the incident point of oblique shock CG to be situated in the Mach reflection region and bistable region, respectively.

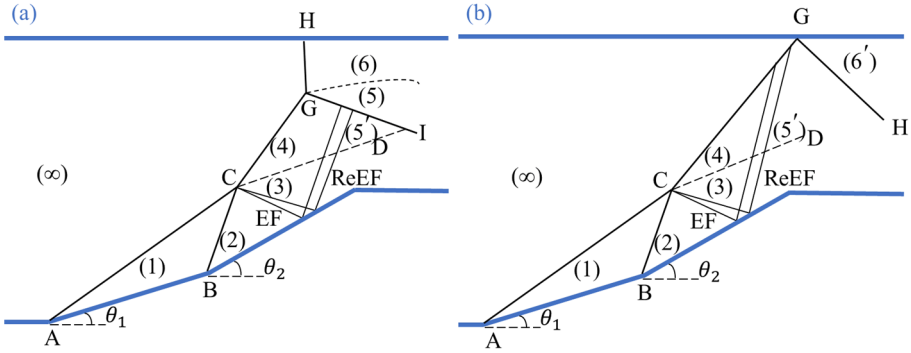

Figure 1. Schematic of Type VI Interference Field in Confined Space Double Wedge Configuration.

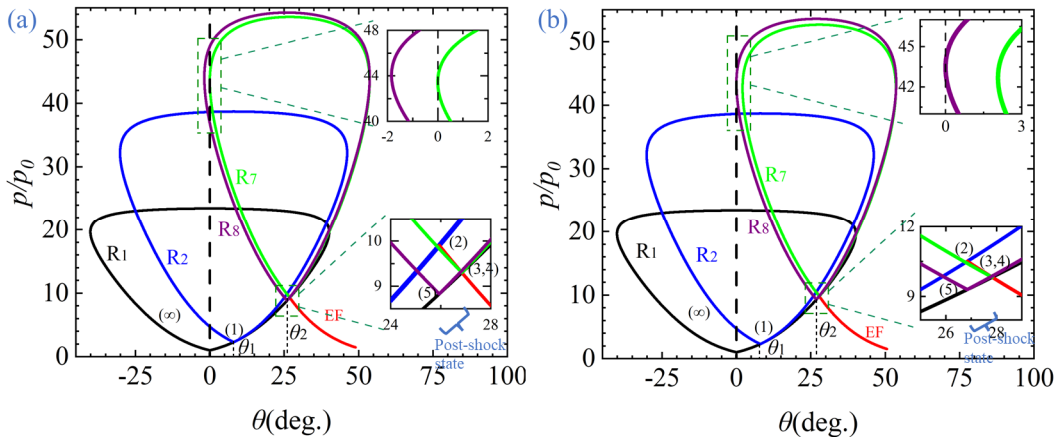

Figure 2. When Ma=4.5, θ_1=8°, the shock polar diagrams depict the criteria for detachment of the expansion wave front/back (a)(b).

Through shock polar analysis, as θ_2 increases, curved line EF starting from Point (2) will increase in θ. The expansion wave exhibits stronger suppression of MR. ReEF can suppress MR under conditions: Ma=5.0, θ_2=27°, Ma=5.5, θ_2=27.5° and Ma6.0, θ_2=28°.

3.2 Numerical validation and flow configuration

In order to check the theoretical analysis, previous theoretical studies have indicated the theoretical potential of expansion waves and shock waves at the triple point to either inhibit or promote the

occurrence of MR on the opposite sidewall. To further elucidate the influence of expansion waves and shock waves on the reflection types on the opposite sidewall and their roles in the evolution of the flow field, a numerical computation is performed under different C_r.

Two solvers were initially used, rhocentralFoam and blastFoam. In the Sod verification case, blastFoam demonstrated accuracy in capturing shock/expansion fans and the precision of numerical methods.

Figure 3 illustrates the pressure contour and zoomed-in views at certain typical snapshots C_r=2.21. The EF emitted from the triple point disturbed by Type VI shock interferes with the reflected shock from the OSW3 on the opposite sidewall downstream of the reflection point, as shown at t=0.36-37 ms in Figure 3(a)(b). The ReEF cannot weaken the strength of the OSW3 on the opposite sidewall. Mach reflection is theoretically admissible based on the analysis in Section 3.1. At t=0.38 ms (Figure 3(c)), following the OSW3, the flow field exhibits a Mach stem and a subsonic region. The Mach stem height continues to increase and remains nearly constant from 5.5 ms to 6.0 ms, signifying the flow field enters a quasi-steady state (Figure 3(d)(e)).

The numerical pressure from Figure 3 ($p_{(1)}$=2.297×10^{4}pa , $p_{(2)}$=9.936×10^{4}pa , $p_{(3)}$=9.331×10^{4}pa , $p_{(4)}$=9.342×10^{4}pa) and the theoretical pressure ($p_{(1)}$=2.296×10^{4}pa , $p_{(2)}$=9.939×10^{4}pa, $p_{(3,4)}$=9.331 ×10^{4}pa) are essentially equal, which verifies the accuracy and feasibility of shock polar analysis.

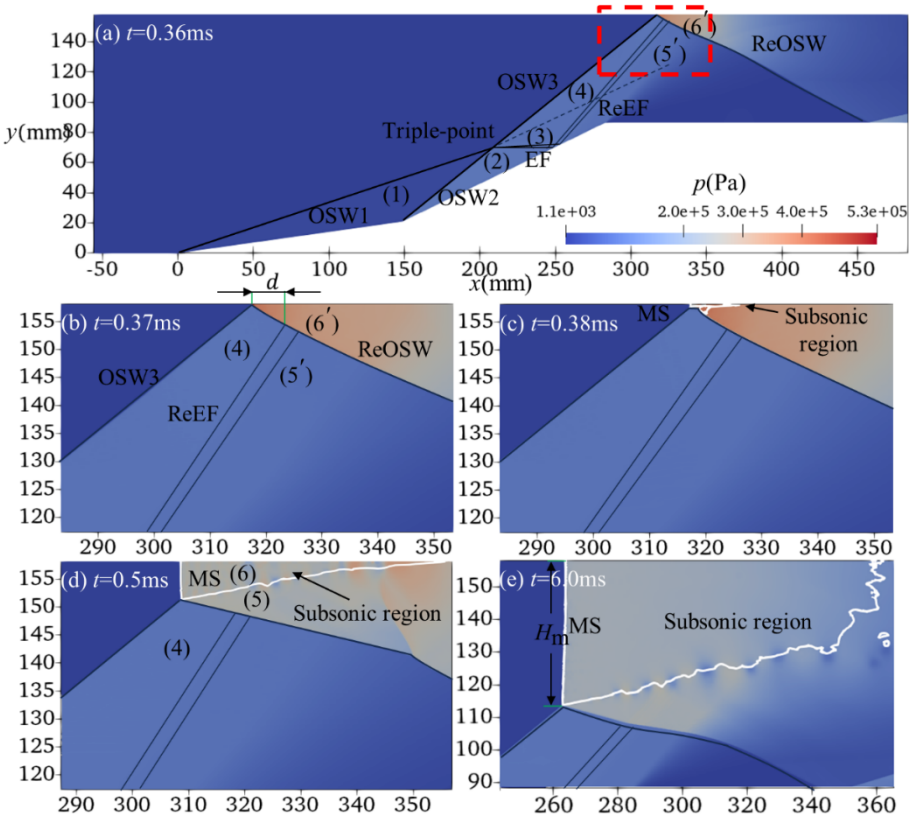

Figure 3. The overall flow field pressure contour plot (a) and enlarged views of local pressure in specific regions (b, c, d, e) at a typical moment when C_r=2.21.

A study of the reflection type of oblique shock before the ReEF aimed to reduce C_r. Figure 4 illustrates the pressure contour and zoomed-in views at certain typical snapshots C_r=1.85. The EF emitted from the triple point disturbed by Type VI shock interferes with the reflected shock from the

OSW3 on the opposite sidewall upstream of the reflection point, as shown at t=0.5 ms in Figure 4(b). The ReEF weakens the strength of the OSW3 on the opposite sidewall. Regular reflection is theoretically admissible based on the analysis in Section 3.1. The OSW3 consistently exhibits regular reflection on the opposite sidewall (Figure 4(c)). The expansion fan at the triple point can suppress the occurrence of MR.

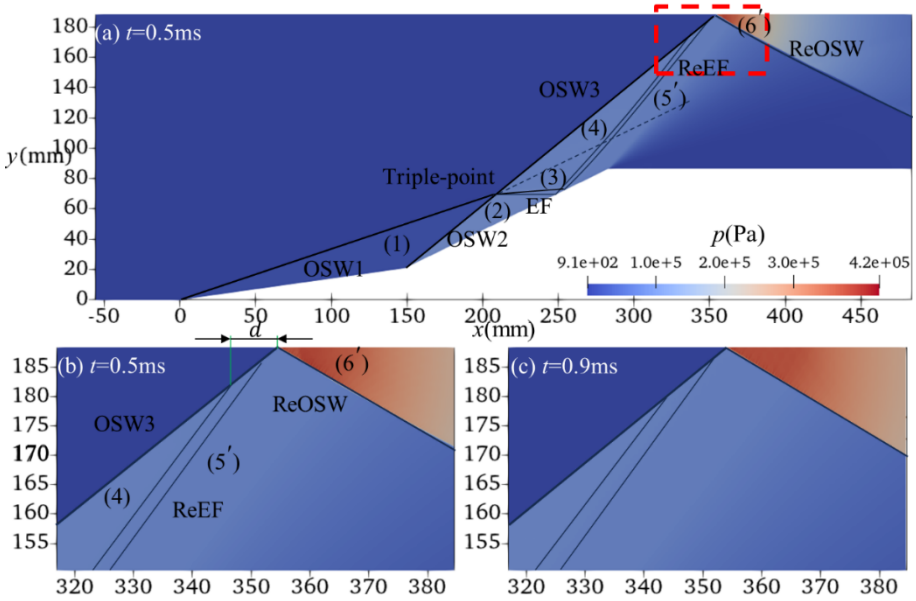

Figure 4. The overall flow field pressure contour plot (a) and enlarged views of local pressure in specific regions (b, c) at a typical moment when C_r=1.85.

4. Conclusion

This paper performs detailed simulations of steady inviscid shock interactions on double-wedge geometries and addresses the impact of expansion waves on reflection types of shock waves in double-wedge configurations. The main conclusions are as follows:

(1) Theoretical analysis of Type VI shock interactions on confined-space double-wedge reveals critical conditions using shock polar theory. Under the operating conditions of Ma=4.5, θ_1=8°, it is observed that there are two critical rear ramp angles corresponding to the reflection of expansion waves at the oblique shock reflection point upstream/downstream. When the rear ramp angle θ_2 satisfies $\theta_{D(4)} < \theta_2 < \theta_{D(5)}$, controlling the contraction ratio can suppress MR occurrence on the opposite sidewall induced by oblique shocks.

(2) Numerical calculations show pressures nearly identical to those from shock polar analysis, validating its accuracy and feasibility.

Acknowledgments

This work was supported by the Science and Technology Research Program of Chongqing Municipal Education Commission (No. KJQN202200739), the Open Project of the State Key Laboratory of High Temperature Gas Dynamics (No. 2023KF09) and the National Natural Science Foundation of China (No. U2141220).

References

[1] Devaraj M K K, Jutur P, Rao S M V, Jagadeesh G and Anavardham G T K 2020 Experimental investigation of unstart dynamics driven by subsonic spillage in a hypersonic scramjet intake at Mach 6 *Phys. Fluids* **32** 026103

[2] Bai C-Y 2023 Shock reflection with incident shock–wedge trailing-edge expansion fan interaction *J. Fluid Mech.* **968** A21

[3] Olejniczak J, Wright M J and Candler G V 1997 Numerical study of inviscid shock interactions on double-wedge geometries *J. Fluid Mech.* **352** 1–25
[4] Bai C-Y and Wu Z-N 2017 Size and shape of shock waves and slipline for Mach reflection in steady flow *J. Fluid Mech.* **818** 116–40
[5] Edney B 1968 *Anomalous heat transfer and pressure distributions on blunt bodies at hypersonic speeds in the presence of an impinging shock*
[6] Bai C-Y and Wu Z-N 2022 Type IV shock interaction with a two-branch structured transonic jet *J. Fluid Mech.* **941** A45
[7] Sravan K K, Samhams Technologies, Nellore, Andhra Pradesh, India, Sameer A S, and Samhams Technologies, Nellore, Andhra Pradesh, India 2020 NAVIER–STOKES COMPUTATIONS ON TYPE-IVr SHOCK-SHOCK INTERACTION MECHANISM OVER DOUBLE WEDGE (15-60) AT HIGH SPEED FLOWS -*Manag. J. Mech. Eng.* **10** 21
[8] Meng B Q, Han G L, Yuan C K, Wang C and Jiang Z L 2017 Experimental and Numerical Study on Hypersonic Flow over Double-Wedge Configuration *AIAA J.* **55** 3227–30
[9] Lin M and Yang F 2023 Transitional criterion and hysteresis of multiple shock–shock interference *Phys. Fluids* **35** 046110
[10] Peng J, Li S, Yang F, Lin M, Han G and Hu Z 2023 Transitional wave configurations between Type III and Type IV oblique-shock/bow-shock interactions *Chin. J. Aeronaut.* **36** 96–106
[11] Olejniczak J, Wright M J and Candler G V 1997 Numerical study of inviscid shock interactions on double-wedge geometries *J. Fluid Mech.* **352** 1–25
[12] Guan X-K, Bai C-Y, Lin J and Wu Z-N 2020 Mach reflection promoted by an upstream shock wave *J. Fluid Mech.* **903** A44
[13] Guan X-K, Bai C-Y and Wu Z-N 2020 Double solution and influence of secondary waves on transition criteria for shock interference in pre-Mach reflection with two incident shock waves *J. Fluid Mech.* **887** A22